Hydrogeology Journal (2019) 27:669–683
https://doi.org/10.1007/s10040-018-1888-x

PAPER

Groundwater-flow-system characterization with hydrogeochemistry: a case in the lakes discharge area of the Ordos Plateau, China

Guofang Pan[1] · Xiaoqian Li[1,2] · Jun Zhang[3] · Yunde Liu[1,2] · Hui Liang[1]

Received: 26 February 2018 / Accepted: 24 October 2018 / Published online: 15 November 2018

Abstract

Understanding the pattern of regional groundwater circulation is essential for sustainable management of groundwater resources and ecosystems protection. A large-scale basin may develop nested groundwater flow systems including local, intermediate and regional flow systems. Hydrogeochemical tracing may be an effective methodology to identify different groundwater flow systems, considering its routine application in field investigation. This study uses wavy-topography-driven regional groundwater flow in the groundwater-fed lakes area of the northern Ordos Plateau, China, as an example to test the effectiveness of a hydrogeochemical method for groundwater-flow-system characterization. Samples of groundwater from wells with different depths and lake water were collected and analyzed. Hierarchical cluster analysis was conducted using the pH, electrical conductivity, and major ions as the input, which leads to three clusters with distinct geochemical compositions. Considering the hydrochemical characteristics, wells depths, and sampling locations, different groundwater flow systems were identified. Geochemical evolution was affected by processes such as leaching, cation exchange, evaporation and human activities. The relationship between δD and $\delta^{18}O$ indicates that the shallow and deep groundwater were recharged by atmospheric precipitation during the modern time and a past colder period, respectively. The groundwater geochemistry is closely related to groundwater circulation depth within different flow systems, indicated by comparison of geochemical processes among the three clusters. This work highlights a hydrochemical method that can identify nested groundwater flow systems in the lakes discharge area of this large-scale basin and provides a better understanding of the hydrogeochemical evolution from the processes involved in relation to groundwater flow systems.

Keywords Groundwater flow · Groundwater-fed lakes · Hydrogeochemical tracing · Hydrochemistry · China

Introduction

As a crucial source of freshwater on Earth, groundwater plays a vital role in supplying human demands and sustaining the ecological environment (Alley et al. 2002; Boulton 2009). Particularly in semiarid and arid regions where available surface-water resources are scarce, groundwater is of great significant concern, especially where it acts as the only available water resource (Currell et al. 2012; Connor 2015; Sishodia et al. 2017). Mapping and understanding the pattern of regional groundwater circulation is essential for the sustainable management of groundwater resources and ecosystems protection. However, the groundwater flow paths could be complex in a large-scale basin, with many recharge and discharge areas, probably leading to development of a hierarchically nested structure (Tóth 1963; Taraszki 2010), i.e., local, intermediate, and regional flow systems.

Basin-scale conceptual groundwater flow models at different locations and geological settings can be well established using analytical or numerical solutions of groundwater flow based on the vertical distribution of hydraulic potential data (Jiang et al. 2011; Wörman et al. 2006; Mádl-Szőnyi and Tóth

Electronic supplementary material The online version of this article (https://doi.org/10.1007/s10040-018-1888-x) contains supplementary material, which is available to authorized users.

✉ Xiaoqian Li
lixiaoqian@cug.edu.cn

[1] School of Environmental Studies, China University of Geosciences, Wuhan 430074, China

[2] State Key Laboratory of Biogeology and Environmental Geology, China University of Geosciences, Wuhan 430074, China

[3] Key Laboratory for Groundwater and Ecology in Arid and Semi-arid Areas, Xi'an Center of Geological Survey, Chinese Geological Survey, Xi'an 710054, China

2015; Tóth et al. 2016). Such models can clearly show how flow systems distribute groundwater, induced by the undulating water table. Nevertheless, field identification and characterization of groundwater flow systems in the subsurface at basin-scale are still confronted with challenges (Jiang et al. 2018). The effectiveness of methods available for groundwater flow system characterization have been discussed and tested, including surface manifestation of recharge and discharge zones according to topography, soil characteristics and vegetation cover (Freeze and Cherry 1979; Tóth 1966), sampling using packer systems in deep boreholes across a given basin cross-section (Hou et al. 2008), geophysical methods like the magnetotelluric technique (Jiang et al. 2014) and geochemical methods (Tóth 1999; Carrillo-Rivera et al. 2007; Wang et al. 2015, 2016).

Surface manifestation is useful to get an initial impression of flow system distribution, but does not carry key information about groundwater flow paths and circulation depth in the subsurface. Using packer systems is a good way to characterize the vertical variations in head and hydrochemistry and the pattern of basin-scale groundwater circulation; however, the high cost of packer systems restricts its wide application in large-scale groundwater investigations. The magnetotelluric technique could be used to identify different flow systems and hydraulic traps, but relies heavily on the assumptions that variation in bulk resistivity is mainly caused by groundwater salinity, and that apparent salinity of groundwater in different flow systems could differ greatly. Among these methods, hydrogeochemical tracing may be more important in identification of groundwater flow systems, considering its wide and routine application in field hydrogeological investigations.

Groundwater is considered as a geological agent that interacts with the surrounding geological environment and generates various physical and chemical phenomena as a consequence (Tóth 1999). Flow-generated processes within aquifers can result in distinct geochemical compositions of groundwater, which can fundamentally contribute to the understanding of the groundwater flow system. Particularly in the discharge area, groundwater could have preserved all physical, chemical and isotopic information, which provides a better insight into the groundwater flow systems (Carrillo-Rivera et al. 2007; Marchetti and Carrillo-Rivera 2014; Wang et al. 2015, 2016). Therefore, geochemistry of groundwater from different depth wells, interpreted within the prevailing hydrogeological framework, may adequately identify the presence of different flow systems; however, it still remains a challenge to integrate these heterogeneous hydrogeochemical data into one coherent interpretation, and no widely accepted methodology for such data integration exists (Menció et al. 2012; Pavlovskiy and Selle 2015). It is worthwhile to further test and develop the effectiveness and applicability of tracing groundwater flow with hydrogeochemistry at basin-scale.

This study uses a selected typical area across groundwater-fed lakes of the Ordos Plateau as an example where local and regional groundwater flow systems may develop, (1) to explore implications of groundwater grouping for groundwater flow systems based on variation of groundwater hydrogeochemistry from wells with different depths with hierarchical cluster analysis (HCA); (2) to determine the origin of groundwater and geochemical processes affecting groundwater hydrogeochemistry along flow paths; (3) to test the application of the hydrogeochemical method for identifying nested groundwater flow systems in the lakes discharge area of the large-scale basin.

Study area and methods

Study area

The Ordos basin, located to the south of the Yellow River in the arid and semi-arid northwestern part of China (Fig. 1a), is one of the large-scale sedimentary basins in China, where the Cretaceous groundwater aquifer is considered as one of the most predominant aquifers for groundwater exploration (Wang et al. 2004; Qian et al. 2016). The northern Ordos basin, also named the Ordos Plateau, covering an area of around 81,000 km^2, is an independent groundwater system divided by the Baiyu mountains at the southern margin with an elevation range of 1,500–1,800 m above sea level (a.s.l.)—Fig. 1b; Wang et al. (2002); Li et al. (2005); Hou et al. (2006a), (2007).

The elevation of the Ordos Plateau decreases from approximately 1,400–1,500 m a.s.l. in the central Sishi Ridge to 1,100–1,200 m a.s.l. at the eastern, western and northern margins (Yin et al. 2010). The Sishi Ridge and Xizhao Ridge divide the Ordos Plateau into three main groundwater basins which are named according to the major rivers in the basin, i.e. the Dosit groundwater basin, the Molin groundwater basin and the Wuding groundwater basin (Fig. 1b). Numerous inland lakes developed in the Ordos Plateau, 139 of which have a total surface-water area larger than 1 km^2 (Hou et al. 2006b; Wang et al. 2010).

The study area is a selected region with an area of 2,400 km^2 (Fig. 1c), which is located near the Sishi Ridge and where several dunes and lakes have developed in topographic highs and depressions, respectively. The five large lakes within the study area are Dake, Chahan, Subei, Xiaoke and Mukai lakes. The climate is typical continental arid to semiarid. According to monitoring meteorological data in the period 1985–

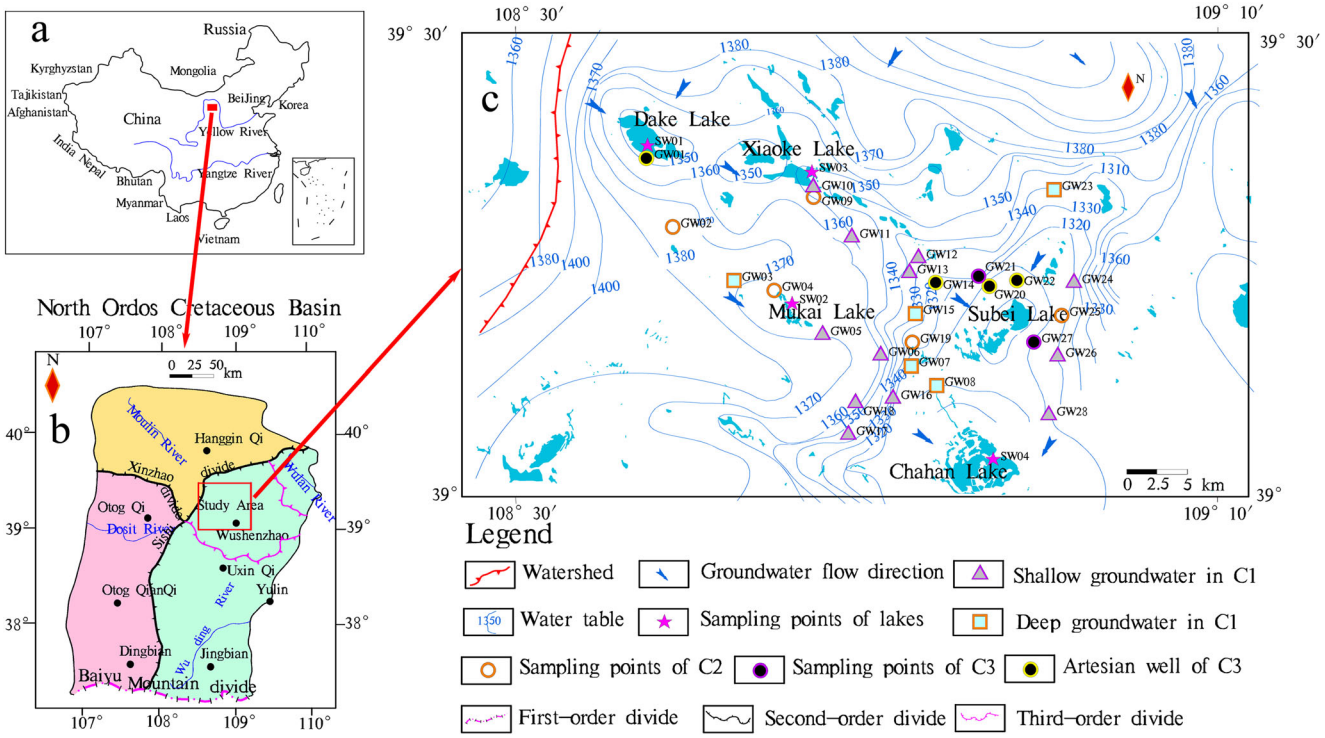

Fig. 1 **a** The location of the Ordos basin in China; **b** a map showing different groundwater systems of the Ordos Plateau and the groundwater systems in the study area; **c** distribution of lakes, sampling locations and contours of the water table elevation (m a.s.l.) in the study area

2008 collected at the Wushenzhao meteorological station, rainfall occurs from March to October, with a mean annual precipitation of 324 mm, while the mean annual potential evaporation is 2,349 mm, measured by a large-diameter evaporation pan E601. The annual average temperature is 6.2 °C, with a daily minimum temperature of −31.4 °C and a daily maximum temperature of 38 °C.

The groundwater system of the study area belongs to the Subei groundwater subsystem of the Wuding groundwater basin in the Ordos Plateau (Yin et al. 2011). The main geological units are poorly consolidated sandstone of the Cretaceous Bao'an Group with a thickness of 700–1,000 m, which is overlain locally by thin Quaternary sediments around the lakes and underlain by the Jurassic mudstone with coal mines. The Cretaceous sandstone and the Quaternary sediments constitute a thick unconfined aquifer system, while the Jurassic mudstone is generally assumed to an aquitard. The Cretaceous sandstones are dominated mainly by quartz, feldspars and albite, with minor quantities of gypsum, halite, calcite and dolomite (Dong 2005; Sun 2010). The Cretaceous aquifer system in the study area from the top down is further divided into the Huanhe and Luohe groups. The groundwater recharge mainly comes from infiltration of precipitation, and slightly from seepage of agricultural irrigation and reservoir and channels. The groundwater discharges by way of potential evaporation, spring overflow, lakes discharge, and artificial extraction.

A hypothesis of groundwater flow systems in the study area

The elevation of the study area ranges between 1,200 m and 1,600 m a.s.l., with the overall terrain relatively higher in the northwest and lower in the southeast (Fig. 2). The Dake, Xiaoke and Mukai lakes are located in regional topographic highs but in local topographic lows, while the Subei and Chanhan lakes are located in regional topographic lows. The groundwater flow driven by the undulating water table is frequently called "topography-driven groundwater flow". The recharge area is always located in topographic highs with high water table, whereas the discharge area is located in topographic lows with low water table. The groundwater-fed lakes are good indicators of groundwater discharge.

The groundwater flow of the study area is topographically controlled, indicated by the inferred water table contours in Fig. 1c showing regional flow from northwest to southeast. The contours of the water table of the study area are closed near the lakes, but nonclosed in topographic highs. The closed contours can imply that the shallow groundwater flows toward the lakes and leads to development of local flow systems, while the nonclosed contours imply that the groundwater in the deep part flows to catchments in the lower reaches and leads to development of regional flow systems (Jiang et al. 2018).

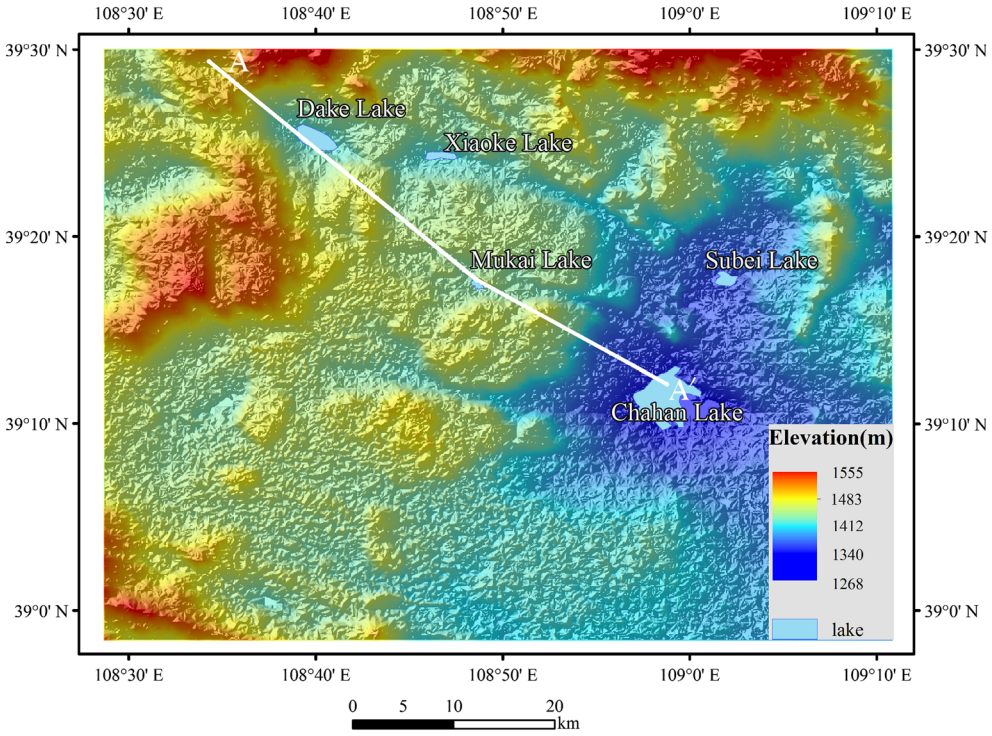

Fig. 2 The digital elevation model (DEM) topographic elevation map of the study area. Also shown is the location of the selected cross-section of A–A′ from the northwestern ridges to the southeastern lakes (see Fig. 3)

According to Tóth's classical model (Tóth 1963), the groundwater-fed lakes may control the groundwater flow system of the basin as an important discharge area of groundwater from local, intermediate and regional flow systems of different circulation depths. The mutually independent local flow system occurs frequently between ridges and neighboring lakes or intermountain depression with shallow circulation depth. The intermediate flow system occurs mostly between the main watersheds and the larger lakes with deep circulation depth. The regional flow system occurs between the major groundwater divides and the large-scale lakes with deeper circulation depth. Therefore, a hierarchically nested groundwater flow systems model of the study area is proposed as shown in Fig. 3, showing subsurface flow paths under a homogeneous aquifer controlled by topography-driven groundwater to lakes.

Hydrogeochemical test methods

Sampling and physiochemical analysis

Twenty eight groundwater samples were taken from wells of different depths in the Cretaceous aquifer operated by local residents for domestic and agricultural irrigation around the lakes in September 2016, together with 4 lake-water samples respectively from the Dake, Mukai, Xiaoke and Chahan lakes. The sample locations are shown in Fig. 1c. The groundwater

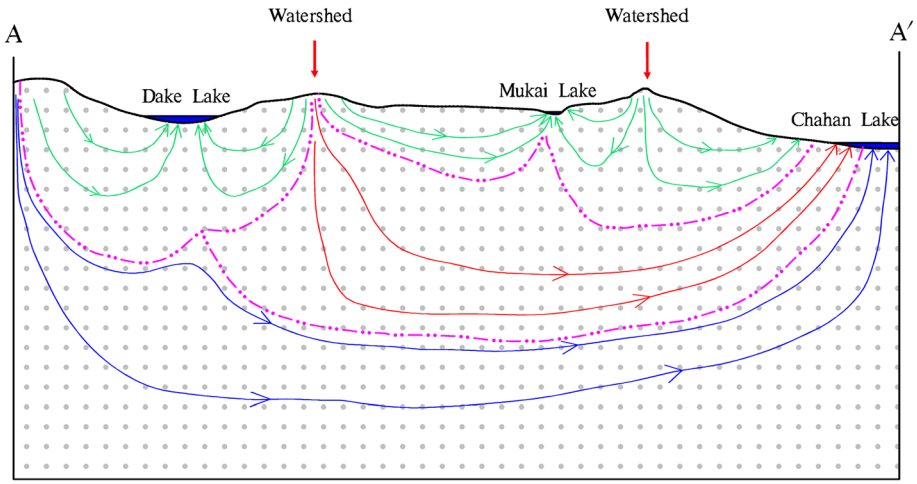

Fig. 3 A schematic figure of the study area showing the development of local, intermediate and regional flow systems controlled by topography-driven groundwater flow to the lakes. The green, red and blue lines with arrows represent local, intermediate and regional flow systems, respectively; the pink dotted lines represent the boundaries of the different flow systems

samples were collected mainly from the Huanhe Group of the Cretaceous aquifer, with sampling wells ranging in depth from several meters to more than 300 m, with groundwater level of approximately 5–15 m. Four deep wells (GW01, GW14, GW20, GW22) are flowing artesian wells, i.e., overflow at the ground surface, at least seasonally. Samples from artesian wells are used to represent deep groundwater in discharge areas, and from nonflowing wells to represent shallow groundwater and deep groundwater in both recharge and discharge areas.

The lake water samples were collected around the lakeside at a depth of ~50 cm. The groundwater samples were taken after removing several well volumes prior to sampling. Parameters, including temperature (T), pH, and electrical conductivity (EC), were measured in the field by a multiparameter portable meter (HACH, HQ40d). Each sample was collected in a 100-ml HDPE screw-cap bottle and sealed tightly to prevent evaporation; the bottles had been precleaned with deionized water in the laboratory and rinsed with abstracted water at least three times before samples were gathered. Each sample was filtered through a 0.45-μm membrane filter while sampling, and the samples for cation concentration analysis were acidified to pH <2 with HNO_3.

The chemical and isotopic compositions of groundwater and lake water samples were determined. CO_3^{2-} and HCO_3^- were determined by routine titrimetric methods within 12 h of sampling. Na^+, K^+, Ca^{2+}, and Mg^{2+} were determined by inductively coupled plasma–optical emission spectrometer (ICP-OES; PE OPTIMA 8300). SO_4^{2-}, Cl^- and NO_3^- were determined by ion chromatography (ICS-900). The analytical precisions of ion concentration measurement are 0.1 mg/L. Charge balance errors (CBE) were calculated for all samples and the majority of the analyses (~94%) presented a CBE <10% except for two samples of 11% for GW20 and 14% for GW04.

The $\delta^{18}O$ and δD in water samples were determined by an isotopic water liquid and vapor analyzer (LGR 920–0032), with a precision of ±0.1‰ for $\delta^{18}O$ and of ±0.5‰ for δD. The stable isotope ratios were expressed in a conventional δ notation, δ_{sample} (‰) = $[(R_{sample} - R_{standard})/R_{standard}] \times 1{,}000$, where R represents the $^2H/^1H$ ratio and $^{18}O/^{16}O$ ratio of the samples and standards, respectively. The results are reported in ‰ relative to the Vienna Standard Mean Ocean Water (V-SMOW) value.

Data analysis for hydrogeochemical tests

The complexity of the source of groundwater in each sample will make the data analysis difficult. The hierarchical cluster analysis (HCA) among the multivariate statistical methods can help to simplify the analysis process. It is an effective way to classify groundwater based on similar hydrogeochemical compositions. The hydrogeochemical processes of the identified groundwater groups can help interpret the relationship between groundwater hydrochemical characterization and flow paths of different flow systems. Additionally, it is also evidenced by the isotopic difference between shallow and deep groundwater, which can trace groundwater origin and indicate groundwater residence time.

Here the ten major physiochemical parameters—pH, EC, K^+, Na^+, Ca^{2+}, Mg^{2+}, HCO_3^-, SO_4^{2-}, Cl^- and NO_3^-—were used for HCA. Since parameters like EC, K^+, Na^+, HCO_3^- and NO_3^- were found to have large skewness according to a normality test, log-transformed standardization of all the parameters was performed in order to lead to smaller skewness and approximate a normal distribution (e.g. Güler et al. 2002). In this way, a new value of each parameter was obtained and used as the input of HCA. Euclidian distance together with Ward's method (Güler et al. 2002) for the nearest neighbor linkage were used to separate different clusters, based on how homogeneous the physiochemical data are, and each variable is weighted equally (Davis 1988). All procedures were conducted using statistical software SPSS19.

Results

Hydrogeochemical characteristics of groundwater and lake water

The groundwater pH ranged between 7.0 and 8.6, indicating neutral to slightly alkaline. The groundwater had total dissolved solids (TDS) concentrations of 219–434 mg/L with an average of 305 mg/L. The concentrations of major ions in groundwater presented large variations: Na^+ (16.5–113.0 mg/L), Ca^{2+} (5.2–141.0 mg/L), Cl^- (9.5–65.2 mg/L), SO_4^{2-} (16.3–116.3 mg/L), HCO_3^- (168–319 mg/L) and NO_3^- (not detected ~113.0 mg/L). Analytical results are given in Table S1 of the electronic supplementary material (ESM).

The HCA results of groundwater samples are shown in the dendrogram of Fig. 4a. Here, a phenon line with a linkage distance of 5 is chosen, which leads to three clusters of the groundwater samples. With larger linkage distances, cluster 1 (C1) and cluster 2 (C2) could combine to one greater group (G1), and cluster 3 (C3) to the other group (G2). The Stiff diagram of average ion concentrations for each cluster (Fig. 4b) clearly shows the similarity and difference of chemical composition among clusters, whose shape reveals the relative proportions of major ions and whose size displays the total concentration (Wang et al. 2015). All the three clusters had similarity on the anion side, mainly dominated by HCO_3^- with varying SO_4^{2-} and Cl^-. However, the cation side shows large difference in dominant cations among the clusters. The C1 and C2 clusters were dominated by Ca^{2+}, whereas C3 was dominated absolutely by Na^+ and K^+. C1 and C2 differed

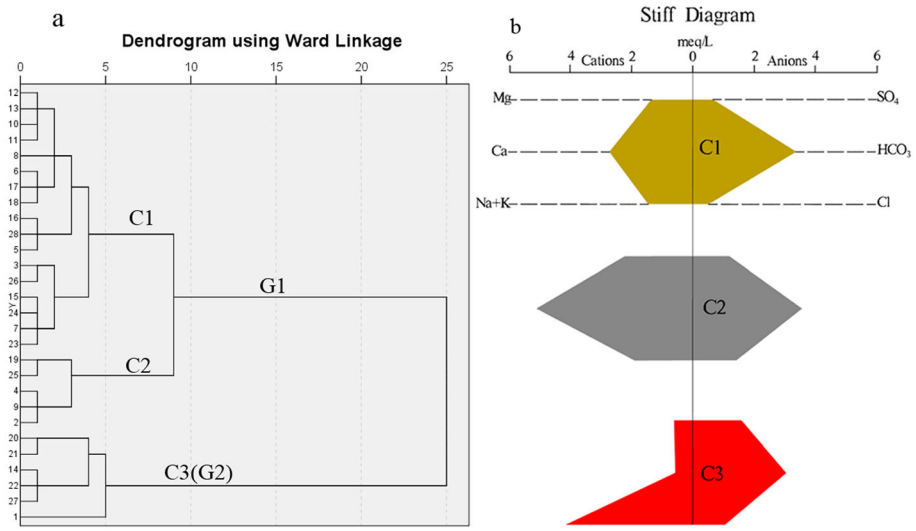

Fig. 4 **a** Dendrogram showing the three clusters, **b** Stiff diagram showing the average ion compositions of each cluster

in concentrations of Ca^{2+}, Mg^{2+} and Na^{+} and K^{+}, with significantly higher Ca^{2+} concentration in C2 than C1.

The physical and chemical compositions for each cluster in groundwater and lake samples are shown in Fig. 5. For different clusters, groundwater chemistry was generally distinct. The lake water pH values were between 8.5 and 9.7 with an average of 9.2, which were significantly higher than groundwater. The lake water was characterized by higher

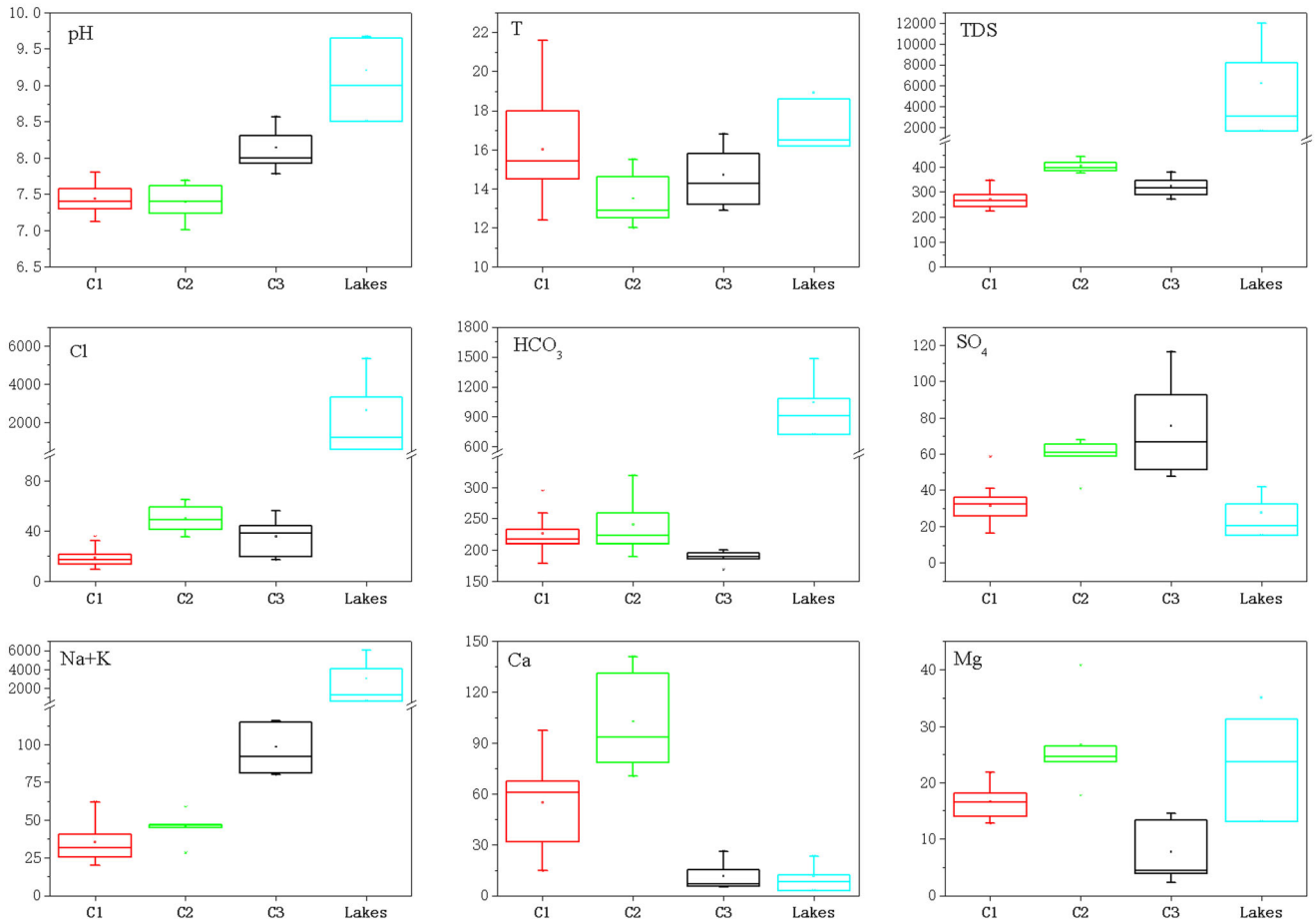

Fig. 5 Box plots of physicochemical indexes of different clusters of groundwater and lake water; all units of ionic concentration are mg/L. The red, green, dark and pale blue boxes represent groundwater of the clusters C1, C2, C3 and lake water, respectively

TDS concentrations, from 1,656 to 12,008 mg/L, with an average of 3,700 mg/L. The lake water basically had higher ion concentrations than groundwater with the exception of Ca^{2+} (3.0–23.3 mg/L) and SO_4^{2-} (15.2–41.9 mg/L). No NO_3^- was detected for lake water samples. The lake water tended to be dominated by Na^+ in cations and HCO_3^- and Cl^- in anions, which is different from the chemical component of saline lakes in other regions.

Hydrogen and oxygen isotopic compositions of groundwater and lake water

The isotopic compositions of groundwater samples ranged from −91.5 to −57.5‰ for δD and from −11.36 to −7.55‰ for $\delta^{18}O$, with an average of −70.7 and − 8.97‰, respectively. The deuterium excesses (d), defined as $d = \delta D - 8\delta^{18}O$, ranged between −6.15 and 6.15‰ with an average of 1.07‰, significantly smaller than the global average of atmospheric precipitation of 10‰. The δD and $\delta^{18}O$ values for lake water were in a range from −60.0 to −43.0‰ with an average of −52.6‰, and from −5.76 to −2.08‰ with an average of −4.48‰, respectively. The deuterium excess of lakes ranged from −26.3 to −8.9‰; hence, the isotopic compositions of lake samples were heavier than those of groundwater, indicating enrichment in ^2H and ^{18}O relative to groundwater.

The groundwater samples in each cluster showed differences in their isotopic compositions. The C2 cluster mostly had higher δD values ranging from −60.9 to −57.5‰ and $\delta^{18}O$ values ranging from −8.38 to −7.55‰, with an average of −58.9 and − 7.93‰ for δD and $\delta^{18}O$, respectively, with the exception of GW19 with −82.8‰ for δD and − 10.32‰ for $\delta^{18}O$. The C3 cluster ranged from −91.5 to −72.9‰ with an average of −79.6‰ for δD and from −11.36 to −8.40‰ with an average of −9.76‰ for $\delta^{18}O$, isotopically depleted relative to C2. The isotopic compositions of groundwater in C1 had a broader range, varying from −85.9 to −61.7‰ and from −10.73 to −7.67‰ for δD and $\delta^{18}O$ values, respectively, which shows a large overlap of C2 and C3. The isotopic averages were − 69.2‰ for δD and − 8.81‰ for $\delta^{18}O$, which were between C2 and C3.

Discussion

The geochemical processes associated with different clusters of groundwater

Groundwater samples in C1, C2 and C3 show distinct hydrogeochemical characteristics that can be used to trace groundwater flow systems. Figure 6 shows the results of the 28 groundwater samples and 4 lake water samples plotted on a Piper diagram (Piper 1953), widely used for finding out the hydrochemical evolution. The C1 cluster is Ca-HCO_3 type water, with a short runoff path. Compared to C1, the C2 cluster has a relatively high concentration for major ions, which may represent just an evolution of C1 water: increasing the flow path enables water–rock interaction (dissolution of more minerals) giving a higher concentration in all ions. The C3 cluster has increasing Na and decreasing Ca + Mg and HCO_3, and this may be the result of ion exchange. The interpretation of the Stiff diagram is completely corroborated by Piper's cation triangle, which clearly demonstrates a relative Mg enrichment between C1 and C2, and a depletion of these two alkali-earth elements in C3, induced by a replacement by alkaline Na. It is noteworthy that Na is the dominant cation in some samples of C1. The lake-water samples were characterized by Cl·HCO_3-Na type.

The Piper diagram clearly shows that the hydrogeochemical evolution sequences are from C1 to C2 or from C1 to C3 and finally end in the lakes. The hydrogeochemical evolution processes indicate that C1 may represent the shallow and deep groundwater at the recharge and runoff areas, while C2 may represent shallow groundwater and C3 may represent deep groundwater at the discharge areas.

A Gibbs diagram (Gibbs 1971), which shows the ratios of $Na^+/(Na^+ + Ca^{2+})$ and $Cl^-/(Cl^- + HCO_3^-)$ versus TDS, is a useful way to identify the genesis mechanisms controlling water chemistry; groundwater may have an assemblage of dissolved loads that reflect dominant effects of rock weathering, evaporation or precipitation in dry regions (Gibbs 1971; Li et al. 2013b). As shown in Fig. 7, all groundwater samples are located in the rock dominance section, with the low ratios of $Cl^-/(Cl^- + HCO_3^-)$ less than 0.3, suggesting that rock weathering controls geochemical evolution of groundwater. The lakes are controlled significantly by evaporation.

From the hydraulic viewpoint, the degree of water–rock interaction is dependent on the flow path and residence time of groundwater in relation to groundwater flow systems. From recharge to discharge areas, various geochemical processes lead to groundwater with different hydrochemical characteristics in recharge and discharge areas (Jiang et al. 2018). The processes controlling groundwater chemistry in the study area are discussed from the perspectives of leaching effect, cation exchange and human activities.

Leaching effect

Weathering of bedrock is one of the main processes controlling the concentrations of chemical constituents in groundwater (Marghade et al. 2012). The leaching effect may be the most important mechanism of rock weathering, which means the transfer of rock minerals into groundwater during the water–rock interaction, resulting in fractional loss of the soluble constituents and a new component added to the groundwater (Yang et al. 2016).

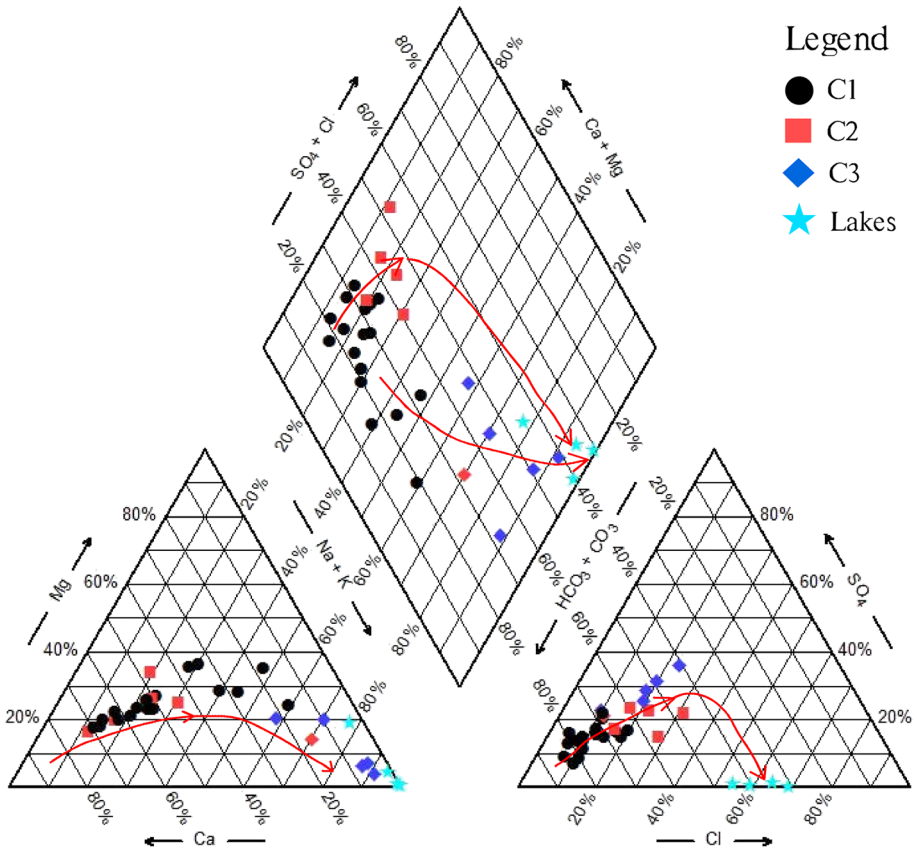

Fig. 6 Piper tri-linear diagram of groundwater and surface water; the red arrows represent the evolution stages of water chemistry types

The processes of leaching can be inferred by the water chemistry, like specific ion relationships. To further refine the geochemical processes of rock weathering, some composition diagrams were derived and these are presented in Fig. 8. The milliequivalent ratios of Na^+ versus Cl^- in Fig. 8a show that most samples are plotted above the 1:1 line, indicating that the dissolution of halite is not the sole source of Na^+ and the Na^+ is also influenced by other processes such as the dissolution of silicates and cation exchange. Only the sample GW02 plotted below the 1:1 line, showing the highest concentrations of Cl^- and NO_3^-; this sample is considered to be influenced by human activities.

The dissolution of gypsum is a major source of Ca^{2+} and SO_4^{2-} in groundwater, indicated by Fig. 8b. All of the samples in C1 and C2 are plotted above the 1:1 line; in contrast, all samples in C3 are plotted below the 1:1 line. Compared to C1 and C2, cluster C3 has relatively high concentration of SO_4^{2-}, indicating that the dissolution of

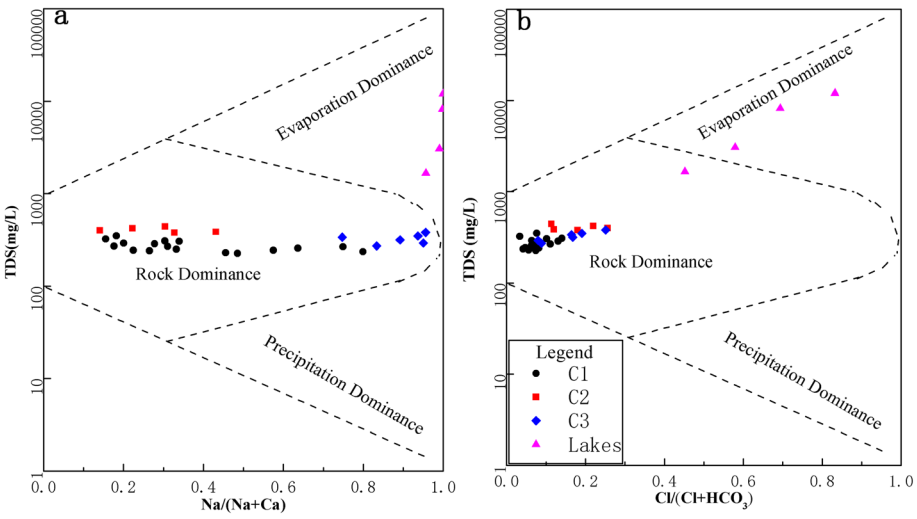

Fig. 7 Gibbs diagrams indicating general mechanisms of groundwater and lakes evolution: **a** Na/(Na + Ca) vs TDS, and **b** Cl/(Cl + HCO_3) vs TDS

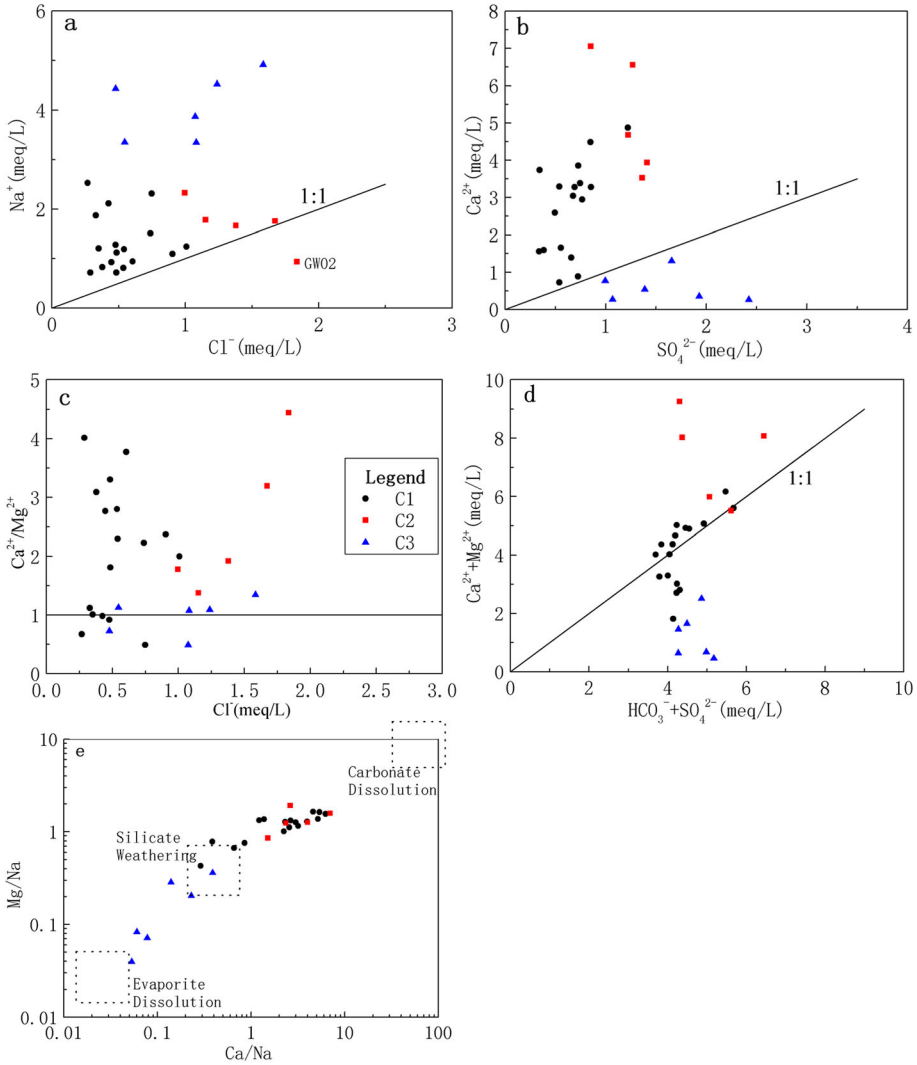

Fig. 8 Plots of the correlations among different ions. Relationships between **a** Cl and Na; **b** SO_4 and Ca; **c** Cl and Ca/Mg; **d** $HCO_3 + SO_4$ and Ca + Mg, and **e** Ca/Na and Mg/Na

gypsum plays an important role. The ratio Ca^{2+}/Mg^{2+} is an important indicator for studying the dissolution of sulfate and carbonate (Yang et al. 2016). Figure 8c shows that most of the samples are plotted above the $Ca^{2+}/Mg^{2+} = 1$ line. $Ca^{2+}/Mg^{2+} < 1$ is caused probably by dissolution of dolomite, and $Ca^{2+}/Mg^{2+} > 1$ suggests that the water–rock interaction in the study area is mainly dominated by the dissolution of calcite (Mayo and Loucks 1995). C3 and some of C1 are plotted near the 1:1 line; however, C2 and most of C1 are plotted above the 1:1 line, indicating the dissolution of calcite and dolomite in C2 and C3, respectively.

Figure 8d shows that the plots of $(Ca^{2+}+Mg^{2+})$ versus $(HCO_3^- + SO_4^{2-})$ fall on both sides of the 1:1 line. The samples in C2 are plotted above the 1:1 line, all samples in C3 are plotted below the 1:1 line, and the samples in C1 are plotted near the 1:1 line, indicating that the weathering of carbonate and silicate minerals contribute most to groundwater chemical components in C2 and the dissolution of sulfate and silicate minerals contribute most to groundwater chemical constituent in C3. With respect to C1, the chemical constituent depends on the weathering of carbonate, sulfate and silicate minerals. The Na-normalized Ca^{2+} versus Mg^{2+} plot (Fig. 8e) further indicates the results of Fig. 8d (Mukherjee and Fryar 2008; Abbas et al. 2015).

When the groundwater is saturated with some minerals, the relevant saturation indices (SI) equal zero; positive values of SI represent oversaturation, and negative values show undersaturation (Smart 1995; Drever 1997). The SIs for gypsum, dolomite, calcite, sylvite and halite were calculated with PHREEQC (Parkhurst and Appelo 1999). The results show that the SI values of gypsum, halite and sylvite for all groundwater samples are less than 0, indicating that evaporite and silicate could practicably be dissolved by the groundwater along the flow path. Most of calcite SI values calculated for the samples in C1 and C2 are greater than 0, indicating the groundwater with HCO_3-Ca type is easily oversaturated. A

few of the SI values for dolomite in all clusters are greater than 0, indicating that the stratum of the study area probably has little dolomite. In addition, almost all of the SI values for calcite and dolomite in C3 are less than 0.

It is considered that the groundwater samples characterized by HCO_3-Ca type are almost oversaturated with respect to calcite; in contrast, the groundwater samples characterized by HCO_3-Na type are undersaturated with respect to calcite and dolomite. The same condition was found in the Dake Lake basin of Ordos Plateau (Wang 2011). Generally speaking, with the groundwater flowing to the discharge area, water–rock interaction will constantly occur, and these minerals may reach an equilibrium gradually.

Cation exchange process

Cation exchange is another vital natural process that can have significant effect on the evolution of groundwater chemistry (Wu and Sun 2016; Li et al. 2013a). A plot of (Ca^{2+}+ Mg^{2+})–($HCO_3^- + SO_4^{2-}$) versus (Na^++ K^+-Cl^-) is widely used to illustrate the possibility that ion exchange influences groundwater compositions (Jalali 2007; Abbas et al. 2015; Amiri et al. 2015). If cation exchange is a noteworthy composition-controlling process, the relation between the two indices should be linear with a slope of −1. As shown in Fig. 9a, most of the samples in C3 are plotted near the 1:1 line; in contrast, the samples in C1 and C2 are located away from the 1:1 line, which indicates the existence of cation exchange in groundwater with HCO_3-Na type.

The chloro-alkaline indices (CAI-1 and CAI-2) proposed by Schoeller (1984) can also indicate the cation exchange (Qian et al. 2016), which can be calculated by the following formulas (Li et al. 2013b):

$$CAI{-}1 = \frac{Cl{-}(Na + K)}{Cl}$$

$$CAI{-}2 = \frac{Cl{-}(Na + K)}{HCO3 + SO4 + CO3 + NO3}$$

where all ions are expressed in meq/L. Negative CAI-1 and CAI-2 indicate the exchange of Ca^{2+} and/or Mg^{2+} in groundwater and Na^+ and/or K^+ in stratum, while positive values of CAI-1 and CAI-2 suggest the exchange of Na^+ and/or K^+ in groundwater and Ca^{2+} and/or Mg^{2+} in stratum. Moreover, the larger the absolute value of CAI-1, the higher the degree of cation exchange. As shown in Fig. 9b, all the values of CAI-1 and CAI-2 except GW02 are negative, indicating that cation exchange results in high concentration of Na^+ and low concentration of Ca^{2+}. Meanwhile, C3 has the higher degree of ion exchange than C2 and C1.

Anthropogenic process

The influence of human activities on the groundwater constituents of the study area primarily includes overexploitation, animal farming and agriculture. These activities may change the condition of groundwater recharge and discharge, and have a complex effect on hydrogeochemical processes. Here, NO_3^- is used as an indicator to trace anthropogenic processes.

NO_3^- is usually regarded as a contaminant from the application of fertilizer. Agricultural activities usually result in non-point source (diffuse) pollution of groundwater and the effects of these practices accumulate with time (Li et al. 2005). As shown in Fig. 10, agricultural activity in the area has affected the groundwater component in C2, which is a result of the traditional flood irrigation and excessive use of fertilizer.

The evolution of hydrochemistry in groundwater and lakes

The hydrochemical types that exist are controlled by lithofacies, and the distributions of the facies are determined by the groundwater flow pattern (Back 1966). A precondition to understanding the evolution of groundwater hydrochemistry is sufficient numbers of samples

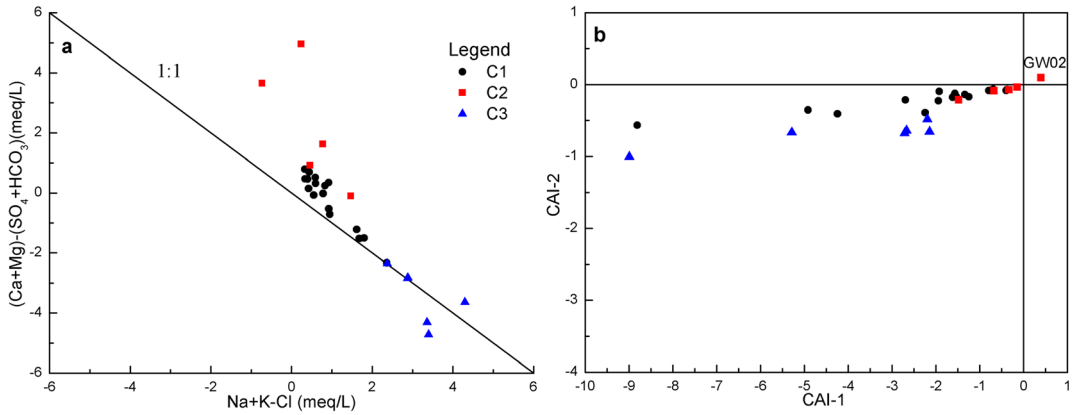

Fig. 9 Bivariate diagrams for studying cation exchange, showing the relationships between **a** Na + K-Cl and (Ca + Mg)–(HCO_3 + SO_4); and **b** CAI-1 and CAI-2. CAI represents Chloric alkali index

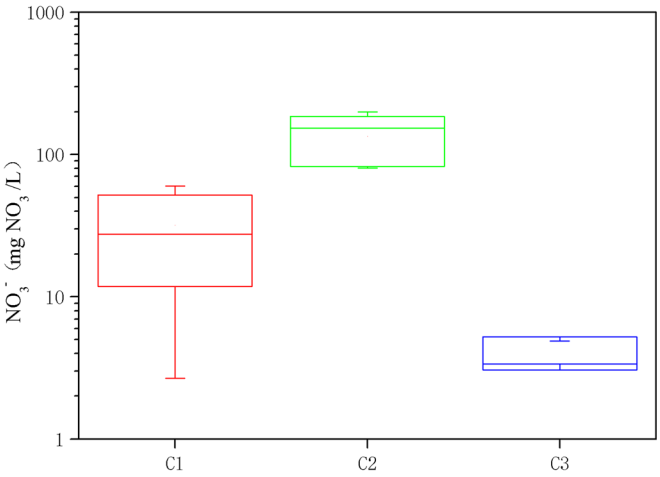

Fig. 10 Diagram of NO_3^- distribution in different clusters of groundwater samples

in both the recharge and discharge areas. In the study area, samples in C2 and C3 are from the shallow wells (depths of 7~60 m) and deep wells (depths >150 m), respectively, which are located in the discharge area near the lakes. Samples in C1 included groundwater from shallow and deep wells (35~360 m) which are located in the recharge area and runoff area.

The groundwater samples in the three clusters showed depth-dependent hydrochemistry, which can indicate that groundwater samples in C1, C2 and C3 belong to different groundwater flow systems. Therefore, the samples characterized by HCO_3-Ca type in C2 and most of C1 are mainly from shallow groundwater of local groundwater systems, and the samples characterized by HCO_3-Na type in C3 and the rest of C1 are mainly from deep groundwater of regional groundwater systems. With respect to hydrochemical evolution processes, from recharge area to discharge area, the hydrochemical types of shallow groundwater in the local flow system are mainly HCO_3-Ca type. Increasing residence time results in higher concentrations of HCO_3 and Ca in the discharge area than the recharge area. The evolution order of deep groundwater in the regional flow system is HCO_3-Ca·Mg (recharge area) → HCO_3-Na·Ca (runoff area) → HCO_3-Na、HCO_3·SO_4-Na (discharge area). For deep groundwater, leaching effect (the dissolution of calcite and silicate rock) and cation exchange is dominant in the recharge and discharge area, respectively. Eventually, both shallow and deep groundwater discharge into the lakes, and significant evaporation makes the hydrochemical type evolve into Cl·HCO_3-Na type.

Groundwater recharge of different flow systems

Groundwater can conserve "fingerprint" isotopic compositions of their origin affected by meteorological processes, which can permit identification of processes like mixing and evaporation, relying on isotopic compositions and their variation. Therefore, the stable hydrogen and oxygen isotopes (δD and $\delta^{18}O$) are used as an ideal indicator to successfully trace groundwater recharge and circulation within different flow systems in many regions (Praamsma et al. 2009; Khalil et al. 2015; Prada et al. 2016; Seraphin et al. 2016).

The δD and $\delta^{18}O$ values of groundwater and lake water samples are plotted in Fig. 11, relative to the local meteoric water line (LMWL, $\delta D = 6.45\delta^{18}O - 6.51$). The LMWL was developed for the northern Ordos basin based on 87 bulk rainfall samples from the six local meteorological stations (Yin et al. 2011). The smaller slope of the LMWL compared with the global meteoric water line (GMWL, $\delta D = 8\delta^{18}O + 10$) reveals the isotopic composition characteristic of atmospheric precipitation in arid and semiarid regions where secondary evaporation during rainfall is expected. Measured groundwater δD and $\delta^{18}O$ values plot adjacent to the LMWL, indicating that groundwater originated from atmospheric precipitation. The analysis of groundwater balance showed that 98.6% of the recharge of groundwater was from precipitation infiltration (Hou et al. 2006b; Yin et al. 2011). The linear regression of groundwater is presented by the equation $\delta D = 7.97\delta^{18}O + 0.84$ ($R^2 = 0.89$). The slope is closer to that of heavy rainfall greater than 40 mm ($\delta D = 7.83\delta^{18}O + 7.28$, Yin et al. 2011), indicating that the groundwater might have originated mainly from heavy rainfall events in the study area. The linear relationship also may imply close hydraulic connection among groundwater at different depths, which is consistent with there being no regional continuous aquitard within the northern Ordos Cretaceous groundwater basin (OCGB).

The lake water samples, however, are scattered on the upper right-hand side, and exhibit a local evaporation line expressed as $\delta D = 3.97\delta^{18}O - 34.82$ (Fig. 11), indicating lake water has experienced a strong evaporation. The intercept of the lakes line and LMWL stands for the original isotopic composition of the recharged rainfall before evaporation (Clark and Fritz 1997; Petrides et al. 2006), which is −80.1‰ for δD and −

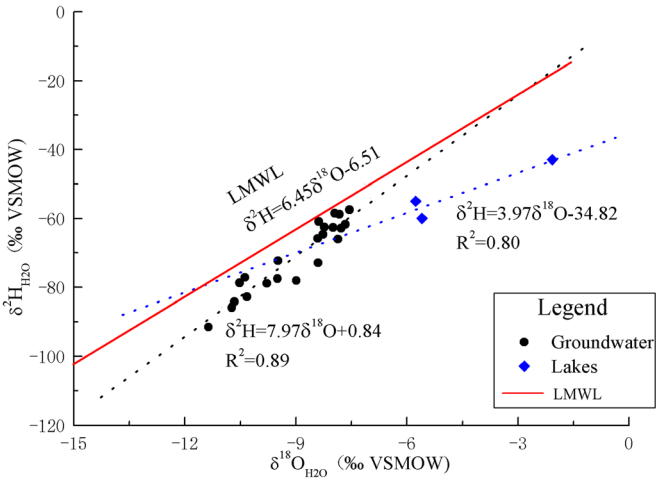

Fig. 11 The relationship between δ^2H and $\delta^{18}O$ for groundwater and lake water; the LMWL represents local meteoric water line, the blue dotted line represents the lake water fitting line, and the black dotted line represents the groundwater fitting line

11.4‰ for $\delta^{18}O$. The lake line also intersects with the groundwater line at −70.2‰ for δD and − 8.9‰ for $\delta^{18}O$, which is between shallow groundwater and deep groundwater, confirming the recharge of the lakes by groundwater. These lakes are perennial lakes located in the discharge zones of regional groundwater flow systems, and thus can receive recharge from local and regional groundwater systems (Winter et al. 2010).

Figure 12 reveals clearly that deep groundwater (wells depth deeper than 150 m) is more depleted isotopically than shallow groundwater with δD < −70‰ and $\delta^{18}O$ < −9‰, although the depths of these sampling wells cannot really represent the actual circulation depths. Almost all groundwater samples of C2 fall in the isotopic range of shallow groundwater (except for GW19), with a linear fitting equation of $\delta D = 4.04\delta^{18}O - 26.85$, whereas groundwater samples of C3 nearly all fall in the isotopic range of deep groundwater (except for GW14), with a linear fitting equation of $\delta D = 5.173\delta^{18}O - 29.09$. Moreover, the intersection of the shallow groundwater line with the LMWL is −60.8‰ for δD and −8.4‰ for $\delta^{18}O$, quite close to the average isotopic values of modern precipitation (δD = −58.5‰ and $\delta^{18}O$ = −8.1‰; Yin et al. 2011). Jiang et al. (2010, 2012) established a relationship between flow systems and groundwater age, pointing out that groundwater in the lower reaches of the basin is young in local flow systems with shallow circulation depth, and is old in regional flow systems with deep circulation depth. The more depleted features reflect that the deep groundwater was recharged during wetter and colder periods than at present, which could correspond to late Pleistocene and early Holocene, implied by ^3H and ^{14}C contents in groundwater (i.e., Yin et al. 2010). It is indicated that the shallow groundwater shows a close connection of modern atmospheric precipitation with a faster circulation rate and shorter circulation path, but the deep groundwater originated from rainfall in the late Pleistocene and early Holocene, with slower circulation rate and longer circulation path.

Conclusions

This study investigated a typical groundwater discharge area of the northern OCGB in the area of lake concentration. Field and analytical measurements for various

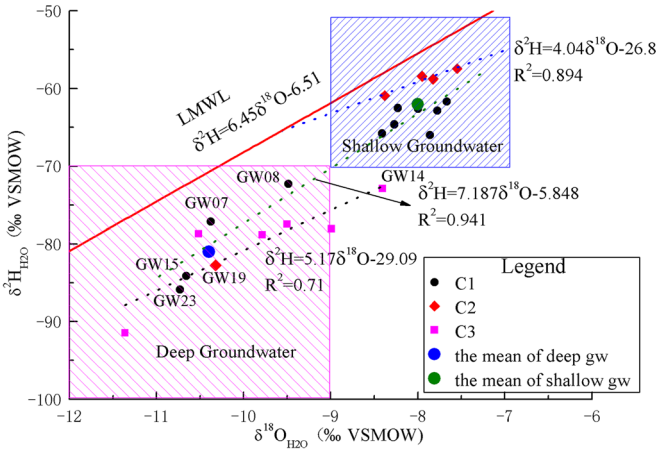

Fig. 12 The relationship between δ^2H and $\delta^{18}O$ for different clusters of groundwater; the red full line represents local meteoric water line, the blue dotted line represents the fitting line of C2, the black dotted line represents the fitting line of C3, the green dotted line represents the fitting line of C1, and gw in the legend means groundwater

physical, chemical and isotopic parameters were carried out for groundwater samples with different depths and lake samples, and the groundwater flow patterns on different scales were identified, including local and regional flow systems.

Shallow groundwater, including clusters C2 and most of C1, was considered to belong primarily to the local flow system. This system was characterized by HCO_3-Ca type with high Ca^{2+} and NO_3^- concentrations, enriched heavy isotopic contents and short flow paths and residence time, with recharge from direct infiltration of modern precipitation and discharge in nearby topographic lows or pumping areas and by evaporation.

Deep groundwater, including cluster C3 and the rest of C1, was considered to belong mainly to the regional flow system with long flow paths and residence time, characterized by HCO_3-Na type with relatively high pH and temperature, high concentration of Na^+, SO_4^{2-} and relatively depleted δ^2H and $\delta^{18}O$, recharged by precipitation during a colder period like the late Pleistocene and early Holocene (Yin et al. 2011). The deep groundwater discharged either through artesian wells or lateral flow, or into lakes far from the recharge area.

Rock weathering is the dominant mechanism controlling the groundwater geochemistry in the study area, and it is affected by processes such as leaching effect, cation exchange, evaporation and human activities. In the lower reach of the basin, groundwater geochemisty is closely related to groundwater circulation depth within different flow systems. The shallow groundwater is dominated by weathering of carbonate and silicate, dissolution of halite and anthropogenic NO_3^- input; the deep groundwater experiences an increasingly stronger degree of water–rock interaction and is dominated by the weathering of silicate, the dissolution of gypsum and halite, and cation exchange.

The lake water, with high concentrations of Na^+, Cl^-, HCO_3^- and EC, is affected by significant evaporation, and the hydrochemical type is $Cl{\cdot}HCO_3$-Na type. The data of δD and $\delta^{18}O$ suggest that lake water located in discharge area is mainly recharged by shallow and deep groundwater from local and regional groundwater systems.

The methodology used in the current study was fundamental to identifying the different groundwater flow systems of this and other large basins and to interpreting the complicated distribution of groundwater hydrochemistry. This work has demonstrated that the hydrochemical method can identify nested groundwater flow systems in the lakes discharge area of a large-scale basin and provides a better insight into the understanding of hydrogeochemical evolution from the processes in relation to groundwater flow systems.

Funding information This study was funded by the foundation of Xi'an Center of Geological Survey, CGS groundwater and ecology key laboratory (No. KLGEAS201602), the National Natural Science Foundation of China (Nos. 41672245 and 41772263), and the Fundamental Research Funds for the Central Universities, China University of Geosciences (Wuhan; No. CUG170644).

References

Abbas Z, Su CL, Tahira F, Mapoma HWT, Aziz SZ (2015) Quality and hydrochemistry of groundwater used for drinking in Lahore, Pakistan: analysis of source and distributed groundwater. Environ Earth Sci 74:4281–4294

Alley WM, Healy RW, Labaugh JW, Reilly TE (2002) Flow and storage in groundwater systems. Science 296:1985–1990

Amiri V, Sohrabi N, Dadgar MA (2015) Evaluation of groundwater chemistry and its suitability for drinking and agricultural uses in the Lenjanat plain, central Iran. Environ Earth Sci 74:6163–6176

Back W (1966) Hydrochemical facies and ground-water flow patterns in northern part of Atlantic coastal plain. AAPG Bull 44(44)

Boulton AJ (2009) Recent progress in the conservation of groundwaters and their dependent ecosystems. Aquatic Conserv Mar Freshwater Ecosyst 19:731–735

Carrillo-Rivera JJ, Varsányi JI, Kovács LÓ, Cardona A (2007) Tracing groundwater flow systems with hydrogeochemistry in contrasting geological environments. Water Air Soil Pollut 184:77–103

Clark ID, Fritz P (1997) Environmental isotopes in hydrogeology. Lewis, Boca Raton, FL

Connor R (2015) The United Nations World Water Development Report 2015: water for a sustainable world, vol 1. UNESCO, Paris

Currell MJ, Han D, Chen Z, Cartwright I (2012) Sustainability of groundwater usage in northern China, dependence on palaeowaters and effects on water quality, quantity and ecosystem health. Hydrol Process 26(26):4050–4066

Davis JC (1988) Statistics, data analysis in geology. Biometrics 44:526–527

Dong W (2005) Application of inverse hydrogeochemical modeling in ^{14}C age correction of deep groundwater in the Ordos Cretaceous artesian basin, MSc Thesis, Jilin University, China

Drever J (1997) The geochemistry of natural waters: surface and groundwater environments. Prentice Hall, Upper Saddle River, NJ

Freeze RA, Cherry JA (1979) Groundwater. Prentice-Hall, Englewood Cliffs, NJ

Güler C, Thyne GD, Mccray JE, Turner KA (2002) Evaluation of graphical and multivariate statistical methods for classification of water chemistry data. Hydrogeol J 10:455–474

Gibbs RJ (1971) Mechanisms controlling world water chemistry. Science 172:870

Hou GC, Lin XY, Su XS, Wang XY, Liu J (2006a) Groundwater system in Ordos Artisan Basin (CAB) (in Chinese with English abstract). J Jilin Univ (Earth Sci Ed) 36(3):391–398

Hou GC, Zhang MS, Liu F, Wang YH (2006b) Groundwater investigation in the Ordos Basin (in Chinese). China Geological Survey, Beijing

Hou GC, Zhang MS, Wang YH, Zhao ZH, Liang YP, Tao ZP, Yang YC, Li Q, Yin LH, Wang XY, Wang D, Li Y (2007) Groundwater resources of the Ordos Basin and its development and utilization (in Chinese with English abstract). Northwest Geol 40(1):7–34

Hou GC, Liang YP, Su XS, Zhao ZH, Tao ZP, Yin LH, Yang YC, Wang XY (2008) Groundwater systems and resources in the Ordos basin, China. J Geol 82(5):1061–1069

Jalali M (2007) Salinization of groundwater in arid and semi-arid zones: an example from Tajarak, western Iran. Environ Geol 52:1133–1149

Jiang XW, Wan L, Cardenas MB, Ge S, Wang XS (2010) Simultaneous rejuvenation and aging of groundwater in basins due to depth-

decaying hydraulic conductivity and porosity. Geophys Res Lett 37: L05403
Jiang XW, Wang XS, Wan L, Ge S (2011) An analytical study on stagnant points in nested flow systems in basins with depth-decaying hydraulic conductivity. Water Resour Res 47:128–139
Jiang XW, Wan L, Ge S, Cao GL, Hou GC, Hu FS, Wang XS, Li HL, Liang SH (2012) A quantitative study on accumulation of age mass around stagnation points in nested flow systems. Water Resour Res 48:W12502
Jiang XW, Wan L, Wang JZ, Yin BX, Fu WX, Lin CH (2014) Field identification of groundwater flow systems and hydraulic traps in drainage basins using a geophysical method. Geophys Res Lett 41: 2812–2819
Jiang XW, Wan L, Wang XS, Wang D, Wang H, Wang JZ, Zhang H, Zhang ZY, Zhao KY (2018) A multi-method study of regional groundwater circulation in the Ordos Plateau, NW China. Hydrogeol J(2):1–12
Khalil MM, Tokunaga T, Yousef AF (2015) Insights from stable isotopes and hydrochemistry to the Quaternary groundwater system, south of the Ismailia Canal, Egypt. J Hydrol 527:555–564
Li PY, Wu JH, Qian H (2013a) Assessment of groundwater quality for irrigation purposes and identification of hydrogeochemical evolution mechanisms in Pengyang County, China. Environ Earth Sci 69:2211–2225
Li PY, Qian H, Wu JH, Zhang YQ, Zhang HB (2013b) Major ion chemistry of shallow groundwater in the Dongsheng coalfield, Ordos Basin, China. Mine Water Environ 32:195–206
Li YF, Xu ZH, Wang JX, Wu YG, Hou GC (2005) Guidelines to locate and protect high-quality groundwater in Baiyu Mountain area of China. Environ Geol 47:647–652
Mádl-Szőnyi J, Tóth Á (2015) Basin-scale conceptual groundwater flow model for an unconfined and confined thick carbonate region. Hydrogeol J 23:1359–1380
Marchetti ZY, Carrillo-Rivera JJ (2014) Tracing groundwater discharge in the floodplain of the Parana River, Argentina: implications for its biological communities. River Res Appl 30:166–179
Marghade D, Malpe DB, Zade AB (2012) Major ion chemistry of shallow groundwater of a fast growing city of central India. Environ Monit Assess 184:2405
Mayo AL, Loucks MD (1995) Solute and isotopic geochemistry and ground water flow in the central Wasatch Range, Utah. J Hydrol 172:31–59
Menció A, Folch A, Mas-Pla J (2012) Identifying key parameters to differentiate groundwater flow systems using multifactorial analysis. J Hydrol 472–473:301–313
Mukherjee A, Fryar AE (2008) Deeper groundwater chemistry and geochemical modeling of the arsenic affected western Bengal basin, West Bengal, India. Appl Geochem 23:863–894
Parkhurst DL, Appelo CAJ (1999) User's Guide to PHREEQC (Version 2): a computer program for speciation, batch-reaction, one-dimensional transport, and inverse geochemical calculations. US Geological Survey Earth Science Information Center, Denver
Pavlovskiy I, Selle B (2015) Integrating hydrogeochemical, hydrogeological, and environmental tracer data to understand groundwater flow for a karstified aquifer system. Ground Water 53:156–165
Petrides B, Cartwright I, Weaver TR (2006) The evolution of groundwater in the Tyrrell catchment, south-central Murray Basin, Victoria, Australia. Hydrogeol J 14:1522–1543
Piper AM (1953) A graphic procedure in the geochemical interpretation of water analysis. United States Geological Survey, Washington, DC
Praamsma T, Novakowski K, Kyser K, Hall K (2009) Using stable isotopes and hydraulic head data to investigate groundwater recharge and discharge in a fractured rock aquifer. J Hydrol 366:35–45
Prada SJ, Cruz V, Figueira C (2016) Using stable isotopes to characterize groundwater recharge sources in the volcanic island of Madeira, Portugal. J Hydrol 536:409–425
Qian C, Wu X, Mu WP, Fu RZ, Zhu G, Wang ZR, Wang DD (2016) Hydrogeochemical characterization and suitability assessment of groundwater in an agro-pastoral area, Ordos Basin, NW China. Environ Earth Sci 75:1356
Schoeller H (1984) Geochemistry of groundwater. UNESCO Studies and Reports in Hydrology 7, UNESCO, Paris
Seraphin P, Vallet-Coulomb C, Gonçalvès J (2016) Partitioning groundwater recharge between rainfall infiltration and irrigation return flow using stable isotopes: the Crau aquifer. J Hydrol 542:241–253
Sishodia RP, Shukla S, Graham WD, Wani SP, Jones JW, Heaney J (2017) Current and future groundwater withdrawals: effects, management and energy policy options for a semi-arid Indian watershed. Adv Water Resour 110
Smart PL (1995) Geochemistry, groundwater and pollution by C.A.J. Appelo and D. Postma, A.A. Balkema, Rotterdam, 1993. No. of pages: xvi + 536. Price: £55.00 (£28 paperback). ISBN 90-5410-106-7. Earth Surf Process Landforms 20:479–480
Sun F (2010) Research on groundwater circulation and environment effect of Dosit River in Ordos Basin. PhD Thesis, Chang'an University, China
Taraszki MD (2010) Book review: Gravitational Systems of Groundwater Flow: Theory, Evaluation, Utilization, by József Tóth (Cambridge University Press, 2009). Hydrogeol J 18:1971–1973
Tóth J (1963) A theoretical analysis of groundwater flow in small drainage basins. J Geophys Res 68:4795–4812
Tóth J (1966) Mapping and interpretation of field phenomena for groundwater reconnaissance in a prairie environment, Alberta, Canada. Int Assoc Sci Hydrol Bull 11(2):20–68
Tóth J (1999) Groundwater as a geologic agent: an overview of the causes, processes, and manifestations. Hydrogeol J 7:1–14
Tóth Á, Havril T, Simon S, Galsa A, Santos FAM, Müller I, Mádl-Szőnyi J (2016) Groundwater flow pattern and related environmental phenomena in complex geologic setting based on integrated model construction. J Hydrol 539:330–344
Wang DQ, Liu F, Hou GC (2002) Groundwater exploration in the Ordos Basin (in Chinese with English abstract). Nor Geol Unders 35(4): 167–173
Wang DQ, Liu ZC, Yin LH (2004) Hydrogeology features and groundwater systems in the Ordos Basin (in Chinese). Quatern Res 25(1): 6–13
Wang H, Jiang XW, Wan L, Han G, Guo H (2015) Hydrogeochemical characterization of groundwater flow systems in the discharge area of a river basin. J Hydrol 527:433–441
Wang JL, Jin MG, Lu GP, Zhang DL, Kang FX, Jia BJ (2016) Investigation of discharge-area groundwaters for recharge source characterization on different scales: the case of Jinan in northern China. Hydrogeol J 24:1–15
Wang WL, Yang GY, Wang GL (2010) Groundwater numerical model of Haolebaoji well field and evaluation of the environmental problems caused by exploitation (in Chinese). South-to-North Water Transf Water Sci Technol 8:36–41
Wang XY (2011) Research on groundwater circulation and hydrochemical evolution in Dake lake watershed in Ordos Basin. MSc Thesis, Jilin University, China
Winter TC, Rosenberry DO, Labaugh JW (2010) Where does the ground water in small watersheds come from? Ground Water 41:989–1000
Wörman A, Packman AI, Marklund L, Harvey JW, Stone SH (2006) Exact three-dimensional spectral solution to surface-groundwater interactions with arbitrary surface topography. Geophys Res Lett 33:L07402
Wu JH, Sun ZC (2016) Evaluation of shallow groundwater contamination and associated human health risk in an alluvial plain impacted

by agricultural and industrial activities, mid-west China. Exposure Heal 8:311–329

Yang QC, Li ZJ, Ma HY, Wang LC, Martín JD (2016) Identification of the hydrogeochemical processes and assessment of groundwater quality using classic integrated geochemical methods in the south-eastern part of Ordos basin, China. Environ Pollut 218:879

Yin LH, Hou GC, Tao Z, Li Y (2010) Origin and recharge estimates of groundwater in the Ordos Plateau, People's Republic of China. Environ Earth Sci 60:1731–1738

Yin LH, Hou GC, Su XS, Wang D, Dong JQ, Hao YH, Wang XY (2011) Isotopes (δD and δ 18 O) in precipitation, groundwater and surface water in the Ordos Plateau, China: implications with respect to groundwater recharge and circulation. Hydrogeol J 19:429–443